Original Article

Tregs-derived interleukin 35 attenuates endothelial proliferation through STAT1 in pulmonary hypertension

Naifu Wan[1#], Wuwei Rong[1#], Wentong Zhu[1], Daile Jia[2], Peiyuan Bai[2], Guizhu Liu[3,4], Qiangyou Wan[3,5], Ankang Lyu[1]

[1]Department of Vascular & Cardiology, Ruijin Hospital, Shanghai Jiaotong University School of Medicine, Shanghai, China; [2]Department of Cardiology, Zhongshan Hospital, Fudan University, Shanghai Institute of Cardiovascular Diseases, Shanghai, China; [3]Shanghai Institute of Nutrition and Health, University of Chinese Academy of Sciences, Chinese Academy of Sciences, Shanghai, China; [4]State Key Laboratory of Respiratory Diseases, Guangzhou Institute of Respiratory Health, The First Affiliated Hospital of Guangzhou Medical University, Guangzhou, China; [5]Academy of Integrative Medicine, Shanghai University of Traditional Chinese Medicine, Shanghai, China

Contributions: (I) Conception and design: N Wan, D Jia, P Bai; (II) Administrative support: A Lyu, G Liu; (III) Provision of study materials or patients: N Wan, W Zhu; (IV) Collection and assembly of data: N Wan, W Rong; (V) Data analysis and interpretation: N Wan; (VI) Manuscript writing: All authors; (VII) Final approval of manuscript: All authors.

[#]These authors contributed equally to this work.

Correspondence to: Ankang Lyu, PhD. Department of Cardiology, Ruijin Hospital, Shanghai Jiaotong University School of Medicine, 197 Ruijiner Rd, Shanghai 200025, China. Email: lvankangrj@163.com.

Background: To explore the source, the role and the specific mechanism of IL-35 and its downstream molecules in the development of pulmonary hypertension.

Methods: 8–10 weeks male mice were undergoing hypoxia combined with SU5416 (HySu) to establish a pulmonary hypertension (PH) model. The phenotype of PH mice was measured by immunohistochemistry and immunofluorescence staining. The levels of two subunits (EBI3 and p35 subunits) in lung tissue were measured by real-time PCR and western blotting. EBI3 monoclonal antibody was administrated as IL-35 neutralization to offset systemic IL-35 expression. Fludarabine, an inhibitor of STAT1 (signal transducer and activator of transcription 1) was used to clarify the role of STAT1 under IL-35 treatment.

Results: After pulmonary hypertension, the expression of IL-35 and its two subunits (EBI3 and p35 subunits) in lung tissue were significantly increased. And the two subunits of IL-35 are highly expressed in Treg cells. Compared with the controlled PH mice, the IL-35 neutralization PH mice showed aggravated pulmonary hypertension phenotype. The specific manifestations are the increase of right ventricular systolic pressure (RVSP), the growing proportion of right heart [RV/(LV+S)], and the remodeling of pulmonary blood vessels increases. The expression of pulmonary vascular endothelium (CD31) in PH mice increased, and the proliferation ability of vascular endothelium enhanced after IL-35 was inhibited. IL-35 phosphorylates STAT1 through the receptor GP130 on pulmonary vascular endothelial cells, which in turn inhibits endothelial cell proliferation. IL-35 recombinant protein can reduce the expression of CD31 in lung tissues of PH mice. But the administration of STAT1 inhibitor made it invalid from the IL-35 effect of reversing pulmonary hypertension.

Conclusions: Tregs-derived IL-35 can reverse the remodeling of pulmonary blood vessels and alleviate the progression of pulmonary hypertension by reducing the proliferation of endothelial cells.

Keywords: Pulmonary hypertension (PH); cardiovascular disease

Submitted Mar 29, 2021. Accepted for publication Apr 29, 2021.
doi: 10.21037/atm-21-1952
View this article at: http://dx.doi.org/10.21037/atm-21-1952

Introduction

Pulmonary hypertension (PH), is a complicated and fatal cardiovascular disease, symbolized by progressive pulmonary vascular remodeling after an elevation of pulmonary arterial pressure of more than 20 mmHg (1). The pathogenesis of PH involves a complex series of processes during which the dysfunction of endothelial cells (ECs) (2), hypertrophy of vascular smooth muscle cells (SMCs), and perivascular infiltration of inflammatory cells may play crucial roles (3). For clinical management of pulmonary hypertension, concerns about clinical symptoms, quality of life, and survival time of PH patients have been used to justify the rapid development of targeted therapies (4). The currently approved drugs mainly include targeted drugs that act on different targets in the three classic pathways of prostacyclin, nitric oxide (NO) and endothelin, but they are all weak antiproliferative agents and are not effective reverse vascular remodeling. So far, no specific medicine has been found to treat the disease, and it is still difficult to escape the fate of lung transplantation at the end stage. And the 5-year mortality rate of patients suffering PH, at 43%, remains low (5). New treatments are urgently needed to effectively avert the pulmonary arterial remodeling present in PH.

Increasing evidence has shown that immunotherapies may play a critical role in managing pulmonary vascular remodeling and targeting immune-related treaties may even ameliorate clinical pulmonary hypertension (6).

Interleukin 35 (IL-35) consists of an Epstein-Barr virus-induced gene 3 (EBI3) subunit and a p35 subunit, is a novel member of the Interleukin-12 family (7), and is an immune-suppressive cytokine, mostly derived from CD3+CD4+CD25hiFoxp3+ regulatory T cells (Tregs). The IL-35 receptor incorporates three diverse dimers, all of which are composed of GP130 and IL-12Rβ2. After being stimulated, the receptor can trigger a downstream signaling through either one of the dimers, which are a heterodimer (GP130 with IL12Rβ2) or a homodimer (GP130 with GP130 and/or IL12Rβ2 with IL12Rβ2) (8). After binding to its receptor, IL-35 can activate and further phosphorylase the signal transducer and activator of transcription (STAT) family members (9). In other cardiovascular diseases, IL-35 has been proven to execute protective functions preventing the cardiovascular system from atherosclerosis erosion and immune inflammation attack after myocardial infarction (10). However, it is far from clear whether IL-35 participates in the pathogenesis or development of PH.

This purpose of this study was to determine whether and how IL-35 participates in pulmonary vascular remodeling after experimentally induced PH. Initially, we assessed serum levels of IL-35 level and two of its ligands, EBI3 and p35, in mice and found these were unregulated in PH. However, ablation of IL-35 markedly aggravated PH mice exposed to chronic hypoxia, by exacerbating pulmonary vascular remodeling and the growth of pulmonary arterial ECs. Further, we showed that IL-35 was expressed mainly in Tregs in the lung tissues after a hypoxia-induced mice model, and exogenous supplying recombinant IL-35 (ReIL-35) protein could ameliorate pulmonary arterial pressure and convert pulmonary vascular remodeling.

We present the following article in accordance with the ARRIVE reporting checklist (available at http://dx.doi.org/10.21037/atm-21-1952).

Methods

Mice

We purchased EBI3$^{-/-}$ and Foxp3^{EGFP} mice from The Jackson Laboratory and crossed them to produce EBI3$^{-/-}$ Foxp3^{EGFP} mice. Wild-type (WT) mice (SLRC Laboratory Animal, Shanghai, China) aged 8–10 weeks were used as experimental controls. Male mice were used in the experiments, given previous reports that estrogens can protect the development of PH through both nongenomic and genomic mechanisms (11). EBI3 monoclonal antibody (MABF848, Sigma-Aldrich) was administrated as IL-35 neutralization, which neutralizes unique IL-35 rather than IL-27, the other known cytokine containing the EBI3 subunit. The antibody was administered by intraperitoneal (i.p.) injection of monoclonal antibody with an initial dose of 100 μg, 50ug additional dose, and a corresponding dose of phosphate buffer saline (PBS) was administered to the control group. Mouse recombinant IL-35 protein (CHI-MF-11135, Chimerigen, Switzerland) was intraperitoneally injected (every other day, 1.5 μg dissolved in 100 μL PBS) to WT mice, against the vehicle group performed 200 μL sterile PBS every other day. To offset the function of STAT1, after ReIL-35 triggered the pathway, Fludarabine (Sigma, 1.5 μg) was used as a STAT1 inhibitor. The mice were exposed to standard nutritious food and fresh sterile water freely and were deposited in an environment retaining controlled temperature (23±1 ℃) and suitable humidity (50%±5%) on a half day light cycle. All animal experiments were performed under a project license granted

by the Animal Ethics Committee of Ruijin Hospital, Shanghai Jiaotong University School of Medicine, China, in compliance with the Animal Ethics Committee of Ruijin Hospital's guidelines for the care and use of animals.

HySu-induced PH mouse model

In the HySu-induced PH model, male mice were utilized to avoid hormonal effects. The 8-week-old male WT mice underwent hypoxia-treated (10% O_2) in a ventilated chamber for 21 days, then randomly received subcutaneously injection of SU5416 (20 mg/kg), a VEGFR2 inhibitor (S8442, purchased from Sigma-Aldrich), every single week under isoflurane anesthesia, as previously described (12,13). The hemodynamic profile was measured at the end point of exposure, as previously described (13,14). Briefly, mice were injected with pentobarbital (30 mg/kg) intraperitoneally in order to anesthetize without offending respiration. A 1.2-F microtip pressure transducer catheter (Millar Instruments, Houston, TX, USA) was then carefully inserted into the right ventricle (RV) to recorded right ventricular systolic pressure (RVSP) for no less than 1 min and the RVSP was captured by a PowerLab data acquisition system (AD Instruments, Sydney, Australia). Mice with HR <250/min were excluded a priori from the analysis (15). After the hemodynamic measurements were completed, the lung vascular system was washed promptly with cold phosphate-buffered saline (PBS), leaving lung sections and heart tissues to be collected. The right ventricle was carefully minced from heart and related the RV and LV, along with the septum (LV+S) were blotted dry, and weighed. The right ventricular proportion was calculated by the weight ratio of the right ventricular wall to the LV and septum [RV/(LV+S), Fulton Index]. All treatments and analyses were performed blinded to the experimental conditions of the animals during hemodynamic measurement and data collection.

Histological analysis

Lungs were extracted from mice and fixed in 10% formaldehyde for no less than 24 h. After fixation, lung tissues were patted dry to plant in a paraffin-embedded container and prepared to be sectioned (5 μm thickness). The lung paraffin slices were then dewaxed and incorporated with hematoxylin and eosin (H&E) staining for histological and imaging analyses. Pulmonary vascular remodeling was quantified using the wall thickness measurement (14,16,17). Around twenty vessels categorized as 20–50 μm (<50 μm) or 51–100 μm (>50 μm) in diameter were captured and ImageJ software (National Institutes of Health, Bethesda, MD, USA) was utilized to calculate wall thickness, presented as a medial area proportion to cross-sectional area (CSA).

Cell culture and isolation

Mouse lung endothelial cells (mLECs) were sectioned and cultured as previously described (14,18) and were carefully separated into 1–2 mm pieces. The pieces were then promptly transported into a sterile container and digested with 10 mL of 1 mg/mL sterile collagenase (Sigma) in a humidly 37 ℃ environment for 1 h. The digested tissues were carefully filtrated through sterile 70-μm cell strainers and twice flushed with warm sterile PBS. The cell suspension was then incubated with anti-CD31-coated Dynabeads (Invitrogen) and the suspension was separated in a magnetic rack. Isolated lung ECs were cultured in endothelial cell medium (ECM) (ScienCell Research Laboratories, Carlsbad, CA, USA) incorporated with 5% FBS (ScienCell Research Laboratories, Carlsbad, CA, USA), and Endothelial Cell Growth Supplement (ECGS) (ScienCell Research Laboratories, Carlsbad, CA, USA). After reaching no less than 80% confluence, cells were again separated with CD102 Dynabeads (BD Pharmingen, San Diego, CA, USA, #553325). For hypoxia exposure in vitro, cells were embedded in culture dishes deposited in a humid and warm tank with 3%O_2/5%CO_2 (16).

Cell proliferation assay

A Cell Counting Kit-8 (Dojindo Laboratories, Kumamoto, Japan) was used to measure cell proliferation, according to the manufacturer's manual. Cells (3×10^4/well) were embedded in 96-well plates, further cultured with indicated treatment and according to the manufacturer's protocol, the remaining medium was removed and replaced by 100 μL fresh medium along with a 10 μL Cell Counting Kit-8 solution. Plates were incubated in a humidified and dark incubator for 1.5 h at 37 ℃ and a SpectraMax 190 Microplate Reader (Molecular Devices) was used to evaluate the absorbances and generate growth curves under 450 nm.

Cell immunofluorescence staining

$CD45^+CD3^+CD4^+CD25^+Foxp3^+$ Tregs, $CD45^+CD11b^+CD64^+$ macrophages, and

$CD45^+CD11b^+CD64^-CD11c^+MHC\ II^+$ dendritic cells were sorted from the lung tissues. Cells were firstly centrifuged in a Cytospin centrifuge (800 rpm, 5 min, Thermo Shandon Cytospin 3) onto Cytospin slides which were air-dried. Fixed cell-slides were then coated in 4% paraformaldehyde (PFA) for no more than 10 min and carefully washed 5 min with sterile PBS three times. After fixation, coated-cells were subjected to a permeabilization with 0.1% Triton X-100 in PBS for no more than 10 min, washed with sterile PBS for 5 min, then embedded with blocking solution for 1 h at room temperature. The plants were then covered with Foxp3 (13-5773-82, eBioscience), CD11c (ab33483, Abcam), CD68 (ab213363, Abcam), p35 (ab131039, Abcam), and EBI3 (sc-166158, Santa Cruz Biotechnology), followed by embedding with secondary antibody (A21208, A32727 and A21094, Invitrogen) for 1 h and incorporated with 4',6-diamidino-2-phenylindole (DAPI) for 5 min.

RNA extraction and real-time PCR

Using TRIzol Reagent (Invitrogen, Carlsbad, CA, USA) total RNA was extracted from lung tissues and mLECs following the manufacturer's protocols. RNA concentrations were assessed by NanoDrop 2000 (Thermo Fisher Scientific, Uppsala, Sweden). RNA samples (1 μg) were reverse-transcribed to cDNA with the Reverse Transcription Reagent Kit (Takara, Dalian, China) and the cDNA was amplified by SYBR Green Universal PCR Mix (Takara, Dalian, China). Target gene expression was normalized to the level of internal control, Glyceraldehyde-3-phosphate dehydrogenase (GAPDH) mRNA. The PCR protocol was as follows: 5 min at 95 ℃ for one cycle, followed by 40 cycles at 95 ℃ for 20 s, 60 ℃ for 30 s, and 72 ℃ for 30 s, along with a final extension at 72 ℃ for 5 min. Related gene expression was measured by the $2^{\Delta\Delta}$Ct method. The primer sequences for PCR are listed as follows: mouse GAPDH 3'→5'-CCCTTATTGACCTCAACTAC ATGGT, 5'→3'-GAGGGGCCATCCACAGTCTTCTG; IL-12Rβ2 3'→5'-AGAGAATGCTCATTGGCACTTC, 5'→3'-AACTGGGATAATGTGAACAGCC; gp130 3'→5'-ATCTTCTCTTGCCTTGGCCT, 5'→3'-AGCTGAAGTTCTCTGGGGTC; p35 3'→5'-AGTTTGGCCAGGGTCATTCC, 5'→3'-TCTCTGGCCGTCTTCACCAT; EBI3 3'→5'-CTTACAGGCTCGGTGTGGC, 5'→3'-GTGACATTTAGCATGTAGGGCA.

Immunofluorescence analysis

Lungs were extracted and embedded in optimal cutting temperature (OCT) compound (Sakura, Torrance, CA, USA), then frozen on the next day. Frozen mice lung sections (7 μm thickness) were then fixed in cold acetone and carefully washed three times with PBS, followed by permeabilization with 0.25% Triton X-100 solution for no more than 10 min, and further embedded with 3% bovine serum albumin (BSA) in PBS for 30 min to offset the non-specific binding site. Additionally, incubation was performed initial covering with the primary antibody overnight at 4 ℃. Signals were embedded and visualized by Alexa Fluor 488, 555, and 633-conjugated secondary antibodies (A21208, A32727, and A21094, Invitrogen) after 2 h incubation at room temperature. The primary antibodies utilized for the experiments were as follows: Foxp3 (1:200; 13-5773-82, eBioscience, San Diego, CA, USA), PCNA (1:200; 2586S, Cell Signaling Technology), CD31 (1:400; ab28364, abcam), EBI3 (1:400; sc-166158, Santa Cruz Biotechnology, Santa Cruz, CA, USA), alpha smooth muscle actin (α-SMA) (1:800; A5228, Sigma-Aldrich), and p35 (1:300; ab131039, Abcam). 4',6-diamidino-2-phenylindole (DAPI, Invitrogen) was used to stain DNA/nuclei and the immunofluorescence images were seized by a laser scanning confocal microscope (Carl Zeiss, Oberkochen, Germany). The $PCNA^+$ PAECs were measured using Image-Pro Plus 6.0 software (Media Cybernetics, Rockville, MD, USA) and further calculated as a proportion of an overall amount of $CD31^+$ PAECs (19,20), while the mPAEC size was quantified as CD31-positive area per cell (16). The measurement of immunohistochemistry was scored independently by two observers.

Western blotting

Proteins from cell and tissue homogenate were extracted with lysis buffer containing protease inhibitors. Bicinchoninic acid (BCA) Protein Assay Kit (Pierce, Thermo Scientific, Waltham, MA, USA), along with the standard protein samples, was used to calculate the total protein concentration and further determined with the BCA method. Lysates containing equal quantities of protein were distributed as indicated and further segregated in 10% sodium dodecyl sulfate-polyacrylamide gel electrophoresis (SDS-PAGE). A polyvinylidene difluoride membrane (Millipore, Billerica, MA, USA) used to transfer, then the

membrane was immersed in 5% fat-free milk dissolved in Tris-buffered saline [150 mM NaCl, 50 mM Tris (pH 7.4)] with 0.1% Tween 20 for 1–1.5 h and embedded at 4 ℃ overnight with primary antibodies against the following proteins: EBI3 (sc-166158, Santa Cruz Biotechnology, Santa Cruz, CA, USA), p35 (ab131039, Abcam), alpha smooth muscle actin (A5228, Sigma-Aldrich), PCNA (2586S, Cell Signaling Technology), p-Stat1 (9167; Cell Signaling Technology, Danvers, MA, USA), p-Stat4 (5267; Cell Signaling Technology), Stat1 (9172; Cell Signaling Technology), Stat4 (2653; Cell Signaling Technology), and GAPDH (5174; Cell Signaling Technology). The membrane was embedded with related horseradish peroxidase-conjugated secondary antibodies (1:2,000; Cell Signaling Technology) dissolved in 5% bovine serum albumin (BSA) solution at room temperature for 1 h and immunoreactivity was then captured by enhanced chemiluminescence reagent (Thermo Fisher Scientific). The blots were then scanned using Tanon Imaging system (Tanon-5200Multi, shanghai, China).

Tregs isolation and adoptive transfer experiments

Mice Tregs were isolated from $Foxp3^{EGFP}$ and $EBI3^{-/-}$ $Foxp3^{EGFP}$ mice. Spleen sections were flushed through a 100 μm cell sieve (352360, Corning, NY, USA) to generate and collect single cell suspension and the cells were then resuspended by supplemented with 2% fetal bovine serum (number 10438026, Gibco). $CD45^+CD3^+CD4^+CD25^+Foxp3^+$ Tregs were selected by flow cytometry under disinfectant. For the adoptive transfer model, the mice were injected via the tail vein with sterile PBS, or 8×10^5 WT $CD45^+$ $CD3^+CD4^+$ $CD25^+$ $Foxp3^+$ Tregs or 8×10^5 $EBI3^{-/-}$ $CD45^+CD3^+CD4^+$ $CD25^+Foxp3^+$ Tregs dissolved in 200 mL sterile PBS 7 days prior to treated hypoxia and SU5416 (21).

Statistical analysis

All statistical data are showed as the mean ± SEM. Data was measured in Prism 7 (Graph Pad Prism Software Inc., San Diego, CA, USA) and Mann-Whitney U test was deployed to compare the mean of two groups. Normal data distribution was examined using Shapiro-Wilk normality test and the means comparison of different groups was performed with the Bonferroni post-hoc test (95% confidence interval). Statistical significance was defined as $P<0.05$ and randomization and blind analyses were used whenever possible.

Results

IL-35 expression elevates in HySu-induced PH mice

IL-35 subunits (EBI3 and p35) mRNA and protein levels were comparatively elevated in lung tissue in HySu-treated mice (*Figure 1A,B*). Additionally, compared with the normoxia group, the lung tissues of HySu-induced mice tended to express higher IL-35 levels (*Figure 1C*) and the serum IL-35 expression also increased in PH mice model based on ELISA analysis (*Figure 1D*). These results suggest IL-35 may participate in the development of PH.

IL-35 mostly derived from regulatory T cells in PH mice

IL-35 has been proven to generate from Tregs and dendritic cells (DCs), and its subunits can express in macrophages. Immunofluorescence staining indicated that the two subunits (EBI3 and p35) were mainly stained in Tregs in mouse lungs after being HySu-induced (*Figure 2A,B*). To further identify the main source of IL-35 after PH, we used FACS analysis sorting out Tregs, DCs, and macrophages from PH mice to detect the co-expression of EBI3 and p35. Interestingly, the two subunits tended to express in Tregs, and comparatively lower p35 subunit expression was seen in macrophages and DCs (*Figure 2B*). To test whether IL-35 positive Tregs participate in the process of PH, wild-type C57BL/6 mice received $CD45^+CD3^+CD4^+Foxp3^+CD25^+$Tregs adoptive transference from $Foxp3^{EGFP}$or $EBI3^{-/-}Foxp3^{EGFP}$ mice spleen 7 days before exposure to hypoxia (Figure S1A,B). Intriguingly, the RVSP and RV/(LV+S) of $EBI3^{-/-}$ Tregs transferred PH mice tended to be higher and the pulmonary vascular remodeling worsened, while WT Tregs transferred PH mice showed a better outcome for symptomatic relief (*Figure 2C,D,E,F*). However, this protective phenomenon from WT Tregs adaptive transference could be averted by further neutralizing IL-35 treatment. All this strengthened the case for the source of IL-35 after PH development and the potentially protective function of Tregs-derived IL-35 after PH.

IL-35 inhibition exacerbates HySu-induced PH and PA remodeling in mice

To further explore the role of IL-35 in PH, we initially

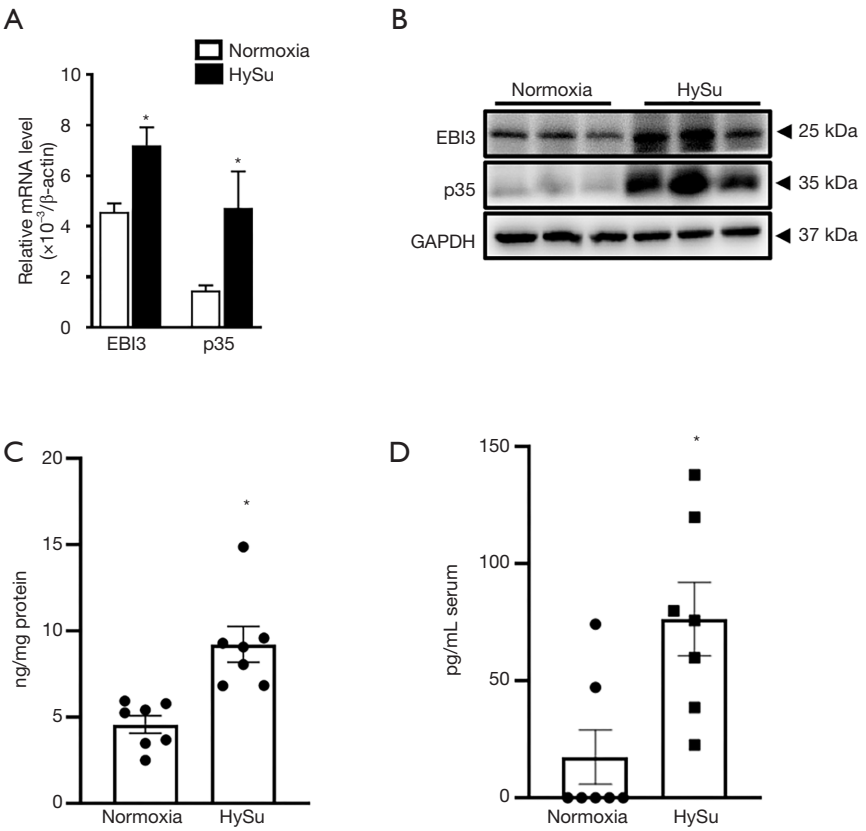

Figure 1 IL-35 expression elevates in HySu-induced PH mice. (A) Relative mRNA levels of EBI3 and p35 were normalized and analyzed from lung tissues in wild-type (WT) mice subjected to normoxia or hypoxia plus SU5416 (HySu). *P<0.05 *vs.* normoxia controls; n=6 per group. (B) Western blotting analysis of EBI3 and p35 levels in lung tissues from WT mice exposed to normoxia or HySu environment. (C) IL-35 generation in lung tissues from WT mice after normoxia or HySu treatment. *P<0.05 *vs.* normoxia controls; n=7 per group. (D) Serum IL-35 contents were measured from normoxia and HySu-induced mice. *P<0.05 *vs.* normoxia controls; n=7 per group. Data represent the mean ± SEM. Statistical significance was evaluated using the Mann-Whitney U test. PH, pulmonary hypertension. HySu, hypoxia plus SU5416.

investigated whether systemic neutralized IL-35 would impact the progression of PH. EBI3 monoclonal antibody (MABF848, Sigma-Aldrich) was administrated as systemic IL-35 neutralization as it uniquely neutralizes IL-35 (7,22,23). Wild-type C57BL/6 mice received HySu for 3 weeks and received treatment with IL-35 inhibition or PBS every week (*Figure 3A*). Intriguingly, IL-35 inhibition dramatically exacerbated the experimental PH mice by developing a significantly higher RVSP and RV/(LV+S) ratio (*Figure 3B*,*C*). Additionally, IL-35 neutralization treatment resulted in a modest aggravation of HySu-induced pulmonary vascular remodeling, evidenced by growing pulmonary vascular wall thickness in both small pulmonary arteries and arterioles (media/CSA), when compared to the PH control group (*Figure 3D*,*E*). These results are consistent with the protective function of Tregs-derived IL-35, indicating that IL-35 inhibition may exacerbate PH development, probably by participating in the pulmonary vascular remodeling.

IL-35 inhibition aggravates lung vascular EC proliferation in PH mice

Pathological lesions, characterized by neomuscularization, proliferated ECs and abnormal perivascular matrix proteins deposition in the development of PH, mainly affect the distal pulmonary arterioles (2,24,25). However, comparison of IL-35 inhibited mice with their counterparts after

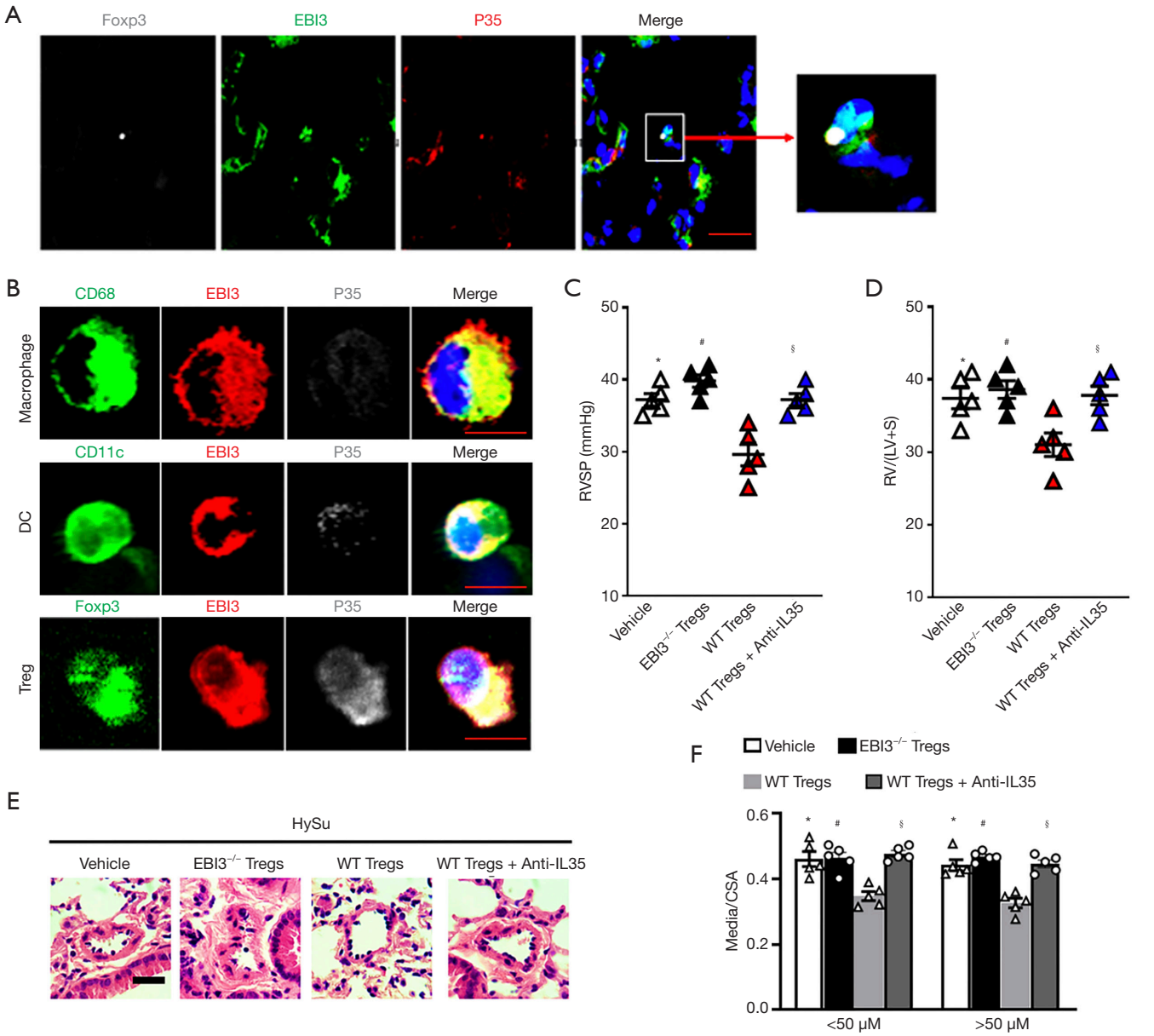

Figure 2 IL-35 mostly derived from Regulatory T cells in PH mice. (A) Immunofluorescence staining of Foxp3 (grey), EBI3 (green), p35 (red), and nuclei (4′,6-diamidino-2-phenylindole, blue) in murine lung tissues after exposure to HySu. Scale bar, 50 μm. (B) Immunofluorescence staining of Foxp3 (green), F4/80 (green), CD11c (green), EBI3 (red), p35 (grey), and nuclei (4′,6-diamidino-2-phenylindole, blue). Scale bar, 5 μm. (C) Right ventricular systolic pressure (RVSP) in vehicle, EBI3$^{-/-}$ mice Tregs transferred, WT mice Tregs transferred, and WT mice Tregs transferred plus IL-35 inhibition mice after HySu exposure. *P<0.05 *vs.* vehicle groups; $^{\#}$P<0.05 *vs.* vehicle groups; §P<0.05 *vs.* vehicle groups; n=5 per group. (D) RV/(LV+S) weight ratio in vehicle, EBI3$^{-/-}$ mice Tregs transferred, WT mice Tregs transferred, and WT mice Tregs transferred plus IL-35 inhibition mice exposed to HySu. *P<0.05 *vs.* vehicle groups; $^{\#}$P<0.05 *vs.* vehicle groups; §P<0.05 *vs.* vehicle groups; n=5 per group. (E) Representative images of H&E staining of lung sections from vehicle, EBI3$^{-/-}$ mice Tregs transferred, WT mice Tregs transferred, and WT mice Tregs transferred plus IL-35 inhibition HySu-induced mice. Scale bar: 20 μm. (F) Quantification of the ratio of the thickness of vascular media to total vessel size (media/CSA) for vehicle, EBI3$^{-/-}$ mice Tregs transferred, WT mice Tregs transferred, and WT mice Tregs transferred plus IL-35 inhibition HySu-induced mice. *P<0.05 *vs.* vehicle groups; $^{\#}$P<0.05 *vs.* vehicle groups; §P<0.05 *vs.* vehicle groups; n=5 per group. Data represent the mean ± SEM. Statistical significance was evaluated using the Mann-Whitney U test. PH, pulmonary hypertension. HySu, hypoxia plus SU5416. RV/(LV+S), weight ratio of the right ventricular wall to the LV and septum. DC, dendritic cells; Treg, regulatory T cells.

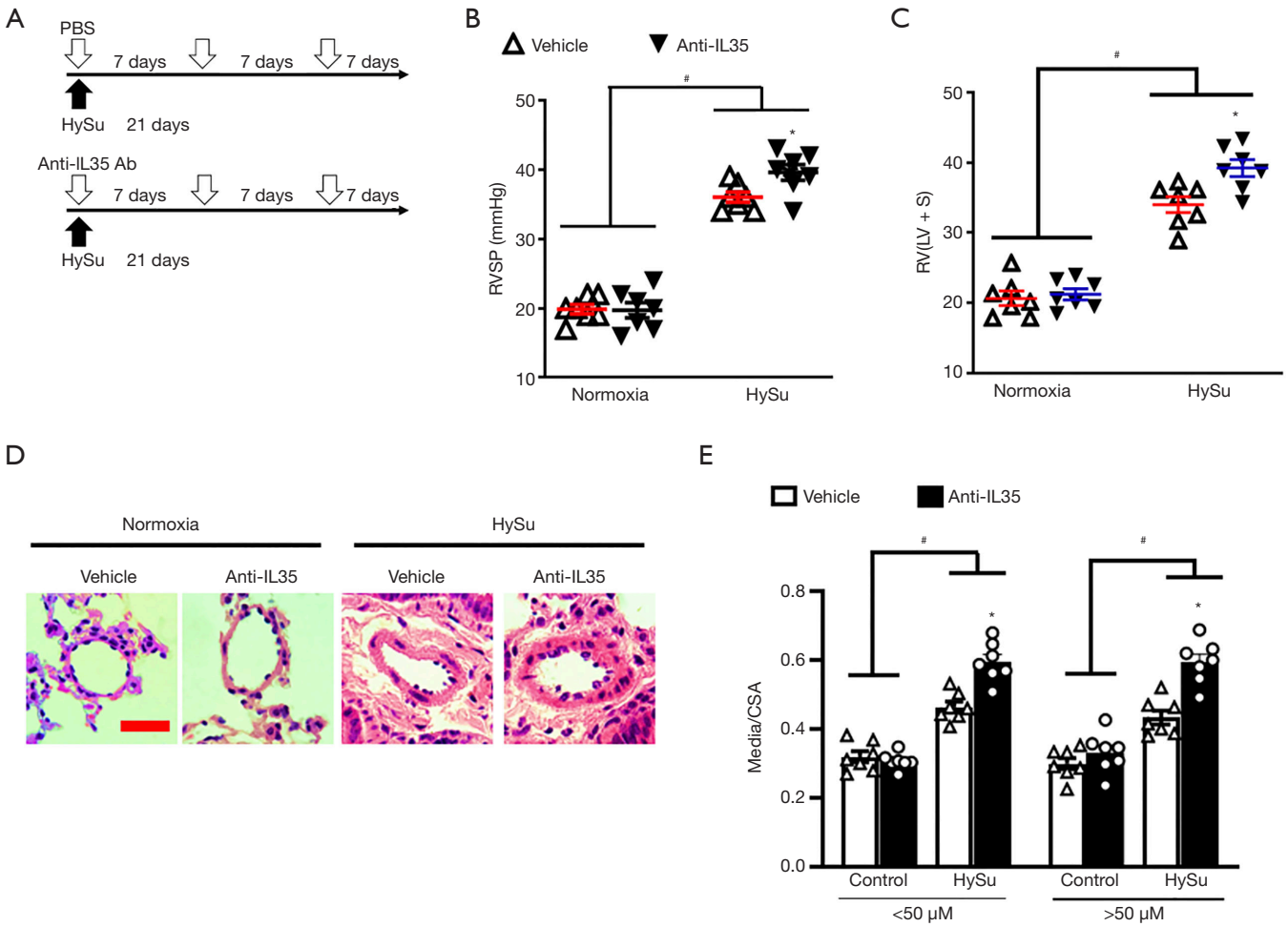

Figure 3 IL-35 inhibition exacerbates HySu-induced PH and PA remodeling in mice. (A) Experimental protocol for administering anti-IL35 or isotype. Mice received intraperitoneal (i.p.) injection of IL-35 neutralizing antibody (initial dose 100 μg, 50 μg additionally dose). (B) Effect of IL-35 mAb administration on right ventricular systolic pressure (RVSP) of HySu-induced mice. #P<0.05 *vs.* normoxia controls; *P<0.05 *vs.* vehicle group; n=7 per group. (C) RV/(LV+S) weight ratio in HySu-exposed PH mice with or without IL-35 inhibition. #P<0.05 *vs.* normoxia controls; *P<0.05 *vs.* vehicle group; n=7 per group. (D) Representative images of H&E staining of lung sections from HySu-induced mice with or without IL-35 mAb administration. Scale bar: 20 μm. (E) Quantification of the ratio of the thickness of vascular media to total vessel size (media/CSA) for HySu-induced mice administered with or without IL-35 inhibition. #P<0.05 *vs.* control; *P<0.05 *vs.* vehicle; n=7 per group. Data represent the mean ± SEM. Statistical significance was evaluated using the Mann-Whitney U test or Kruskal-Wallis tests followed by Dunn test. PH, pulmonary hypertension. PA, pulmonary arterial. HySu, hypoxia plus SU5416. RV/(LV+S), weight ratio of the right ventricular wall to the LV and septum.

HySu-treatment showed there was no significant difference in α smooth muscle actin (α-SMA) expression and α-SMA positive cells, which is a symbol of pulmonary vascular neomuscularization. (*Figure 4A*,*B*). Also, IL-35 inhibition failed to make a significant change to the perivascular matrix proteins deposition in lung of HySu-induced mice, such as collagen-1 (*Figure 4A*). Western blotting analysis and Immunofluorescence staining demonstrated that IL-35 inhibition markedly increased CD31 expression in lung and aggravated HySu-induced lung EC size (*Figure 4A*,*B*). In the PH mice model, staining for CD31 showed that IL-35 inhibition remarkably exacerbated lung EC proliferation by increasing PCNA incorporation rate (*Figure 4C*,*D*). We then tested whether this phenomenon could be replicated in vitro. IL-35 neutralization treatment was used in mLECs (22) and the results showed that the inhibition of

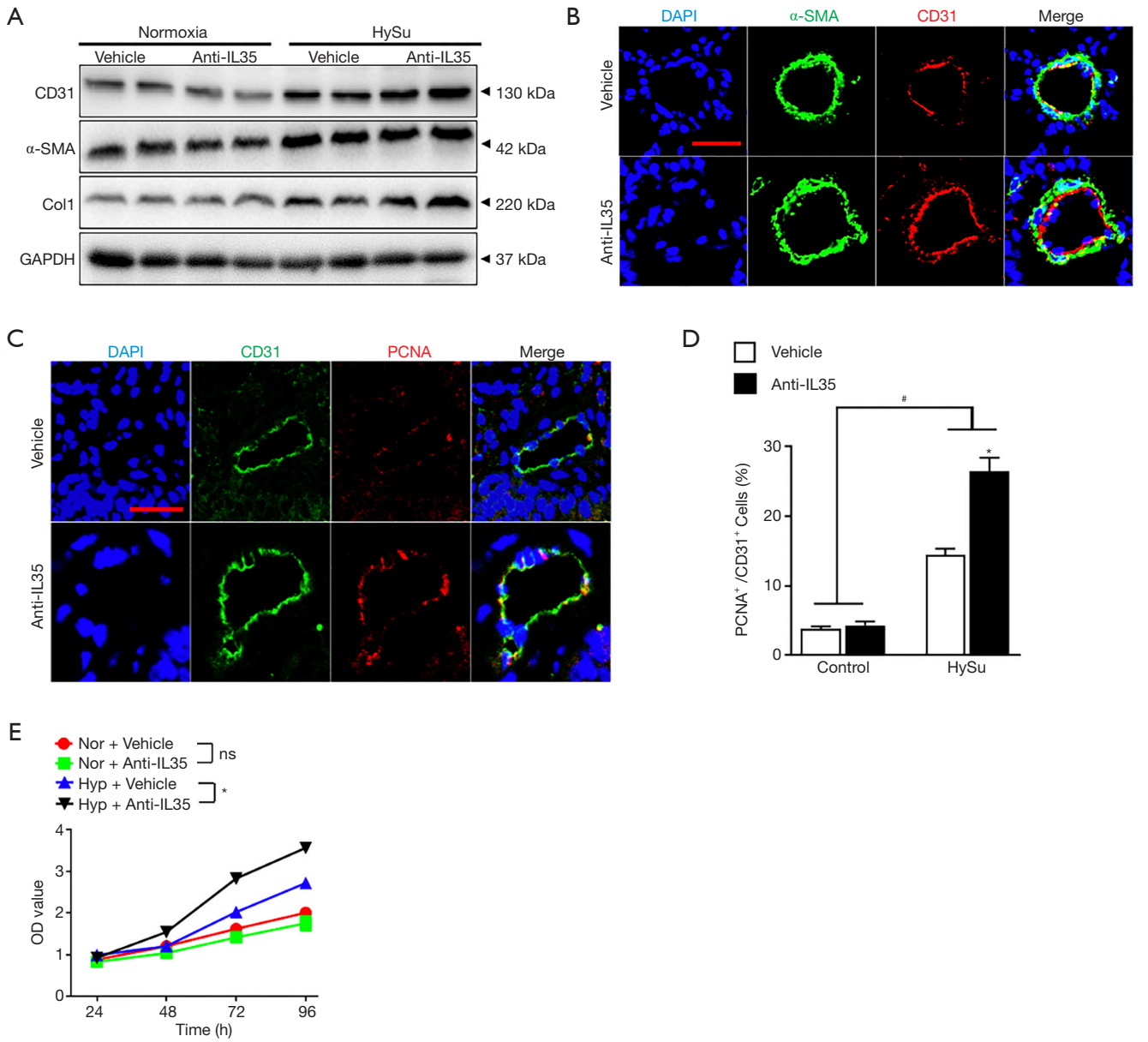

Figure 4 IL-35 inhibition aggravates lung vascular EC proliferation in PH mice. (A) CD31, α-SMA and Collagen I protein expression in the lung tissue isolated from wild-type (WT) and anti-IL35 treated HySu-induced mice; n=6 per group. (B) Representative immunofluorescence analyses of α-SMA and CD31 in the lung tissue of mice with or without anti-IL35 administration after exposure to HySu. Scale bars: 20 μm. (C) Representative immunofluorescence images of CD31 and PCNA in the lung tissue of mice with or without anti-IL35 administration after exposure to HySu. Scale bars: 20 μm. (D) Quantification of PCNA+CD31+ cells in C. #P<0.05 *vs.* normoxia controls; *P<0.05 *vs.* vehicle group; n=7 per group. (E) Effect of blocking IL-35 on the proliferation of hypoxia-exposed mLECs. *P<0.05 *vs.* as indicated; n=6 per group. Data represent the mean ± SEM. Statistical significance was evaluated using the Mann-Whitney U test or Kruskal-Wallis tests followed by Dunn test. PH, pulmonary hypertension; EC, endothelial cell; HySu, hypoxia plus SU5416; Col1, collagen I; mLECs, mouse lung endothelial cells.

IL-35 enhanced hypoxia-induced mLECs proliferation (*Figure 4E*). Thus, inhibited IL-35 exacerbated HySu-induced PH and pulmonary vascular remodeling in mice by aggravating lung vascular EC proliferation.

IL-35 abrogates pulmonary EC proliferation through STAT1

The IL-35 receptor (IL-35R) is made up of IL12Rβ2 and GP130 subunits and IL-35 can trigger downstream in a unique and unconventional way. It can signal down through a heterodimer of both two receptor chains IL12Rβ2 and GP130 (GP130:IL12Rβ2) or homodimers of each single chain (GP130:GP130 and/or IL12Rβ2:IL12Rβ2) (8), and requires STAT1 (downstream of GP130) and/or STAT4 (downstream of IL12Rβ2) to transcription (9). To investigate this we first detected whether these two receptors were present in mLECs and found GP130 was significantly expressed in lung ECs (*Figure 5A*), while IL12Rβ2 expression increased in the mLECs of HySu-induced mice compared to an extremely low level in normoxia mLECs (*Figure 5B*). To detail the mechanism by which IL-35 meditates ECs homeostasis under hypoxic condition, two specific antibodies blocking GP130 or IL12Rβ2 were used in ECs. Interestingly, blocking GP130 interfered with the phosphorylation of STAT1 under IL-35 treatment, further increased PCNA expression after exposure to hypoxia. However, IL12Rβ2 blockage interfered with the phosphorylation of STAT4 after IL-35 stimulation treatment and had no significant influence on PCNA expression under hypoxic conditions (*Figure 5C*). That means, IL-35 interfered PCNA expression only by GP130 receptor in ECs under hypoxia. Given the unconventional mode through which IL-35 is signaled (8), we hypothesized that IL-35 may wield its function by one receptor subunit, GP130, and its downstream STAT1 in ECs. We then used fludarabine (Sigma), a STAT1 inhibitor, to offset the effect of STAT1 after IL-35 triggered the pathway under hypoxia. We found STAT1 inhibition had the same function as GP130 blockage had, which increased expression of PCNA (*Figure 5C*).

Next, ReIL-35 and fludarabine were applied to the PH mice model (Figure S2A). We examined pulmonary hemodynamic and histological changes in HySu-induced mice after IL-35 treatment. As expected, IL-35 significantly attenuated PH by reducing RVSP and RV/(LV+S) (Figure S2B,C). Furthermore, IL-35 treatment tended to modestly suppress HySu-induced pulmonary vascular remodeling in pulmonary arteries, that is, it decreased pulmonary vascular wall thickness (Figure S2D). IL-35 also dramatically suppressed HySu-induced lung ECs by reducing their size (*Figure 5D*). Further immunofluorescence staining showed that IL-35 remarkably inhibited HySu-induced lung proliferation by reducing the PCNA expression rate in CD31 (*Figure 5E,F*). This could also be seen in the *in vivo* phenotype as the decreased proliferation ability of mLECs under IL-35 treatment after exposure to hypoxia (*Figure 5G*). Indeed, these beneficial phenotypes from IL-35 could be abolished by blocking STAT1 (Figure S2B,C,D). When compared to IL-35 treatment PH mice, mice further undergoing STAT1 blockage developed severe PH, just as vehicle PH mice, and when exposed to hypoxia, the inhibition ability of IL-35 to suppress ECs proliferation could not be observed when STAT1 was blocked. These results indicate IL-35 abrogates HySu-induced mice by triggering GP130 and the STAT1 signaling pathway in ECs.

Discussion

Current therapies for PH are mainly designed to slow the progression of vascular remodeling focus on releasing the pulmonary vasculature temporarily in sync with reducing pulmonary arterial pressure (4). However, little attention has been paid to changing pulmonary vascular immune conditions and averting related vascular remodeling disorders in the long run. Therefore, a deeper understanding of disorders of immune regulation in PH would assist current therapies to a more productive level and potentially benefit novel drug R&D in the treatment of PH.

Cytokines in the pulmonary microenvironment play essential roles in pulmonary vascular remodeling, such as triggering the hypertrophy of pulmonary vascular smooth muscle cells and attracting infiltrated immune cells. The Interleukin-12 family was discovered in 2007, and Interleukin-35 is a new member of it (7). Recent studies have investigated the connection between impaired immune regulation and pulmonary endothelium, which is required for pulmonary vascular local homeostasis (26). Under physiological conditions, IL-35 expression was absent or present only at very low levels in the cardiovascular system. However, under stress conditions such as ischemia, hypoxia, hyperlipidemia, and an acidic environment, upregulated IL-35 displayed significantly higher activities (27,28). Our HySu-induced PH mice model involves hypoxic stress and

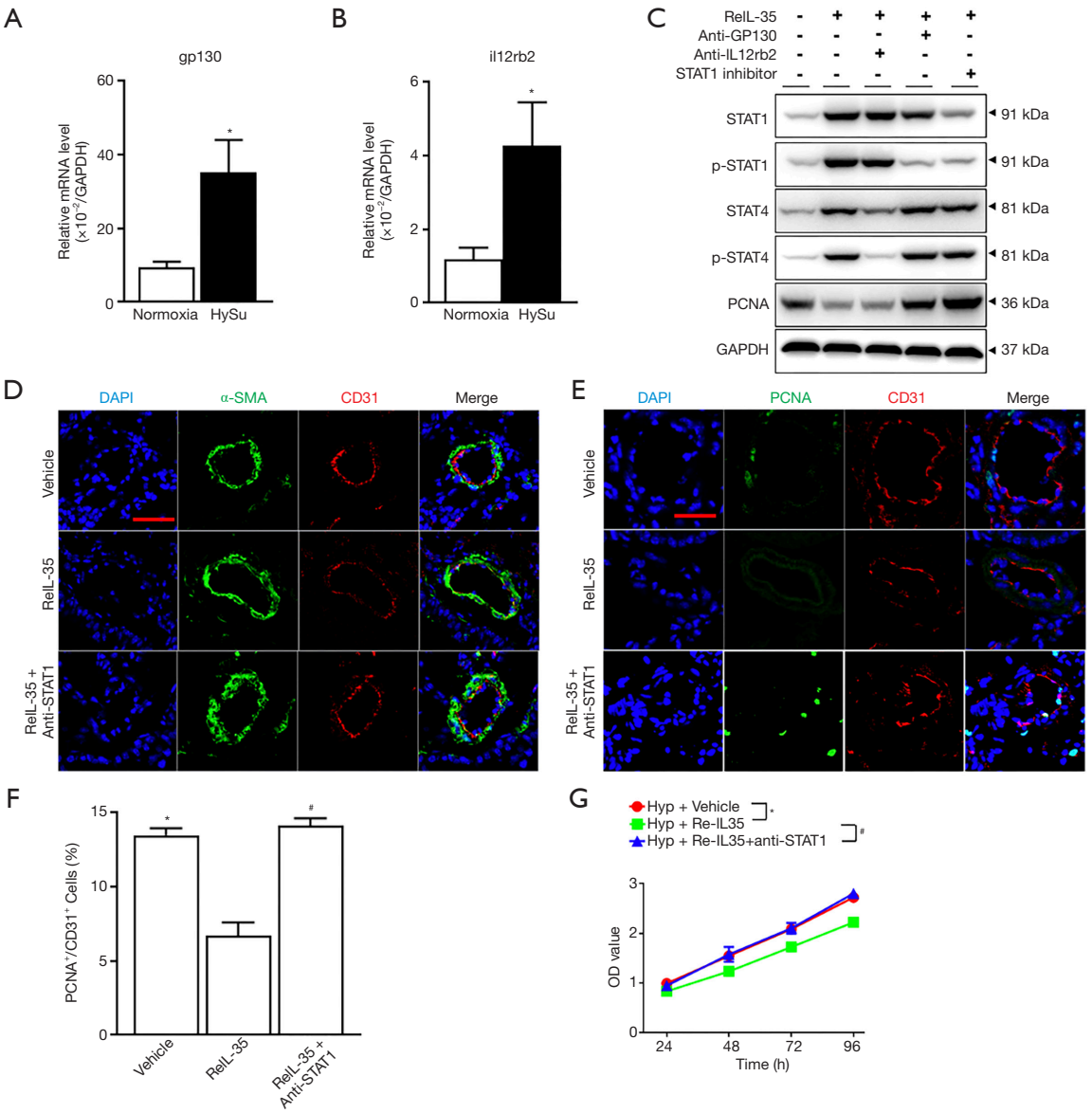

Figure 5 IL-35 abrogates pulmonary EC proliferation through STAT1. (A) Relative mRNA levels of gp130 in mLECs extracted from lung tissues of normoxia or HySu-induced mice. *P<0.05 *vs.* normoxia controls; n=6 per group. (B) Relative mRNA levels of il12rb2 in mLECs extracted from lung tissues of normoxia or HySu-induced mice. *P<0.05 *vs.* normoxia controls; n=6 per group. (C) Indicated proteins level of HUVEC, which were pretreated with or without the anti-GP130 antibody (100 ng/mL), anti-IL12Rb2 antibody (2 mg/mL), and STAT1 inhibitor fludarabine (2 mg/mL) for 30 min, then cultured with ReIL-35 (100 ng/mL) for 24h under hypoxia. (D) Representative immunofluorescence analyses of α-SMA and CD31 in the lung tissue of HySu-induced mice with ReIL-35 administration, without ReIL-35 administration, and with both ReIL-35 and STAT1 inhibition treated. Scale bars: 20 μm. (E) Representative immunofluorescence images of CD31 and PCNA in the lung tissue of PH mice with ReIL-35 administration without ReIL-35 administration and with both ReIL-35 and STAT1 inhibition administrated. Scale bars: 20 μm. (F) Quantification of PCNA+CD31+ cells in E. *P<0.05 *vs.* vehicle group; #P<0.05 *vs.* vehicle group; n=6 per group. (G) Effect of ReIL-35 and both ReIL-35 and fludarabine on the proliferation of hypoxia-exposed mLECs. *P<0.05 *vs.* vehicle group; #P<0.05 *vs.* vehicle group; n=6 per group. Data represent the mean ± SEM. Statistical significance was evaluated using the Mann-Whitney U test or Kruskal-Wallis tests followed by Dunn test. EC, endothelial cell; mLECs, mouse lung endothelial cells; HySu, hypoxia plus SU5416; ReIL-35, recombinant IL-35.

could generate a potential milieu for IL-35 expression, and activation (29), and growing evidence indicates that other Interleukin-12 family members (IL-12, IL-23, IL-27) have participated in cardiovascular diseases (30-32). STAT1 can promote cell proliferation and angiogenesis in tumors (33). Proliferation of pulmonary arterial ECs, which is seen as a harmful consequence of pulmonary vascular remodeling, thereby aggravating the development of PH progression (21,34).

In this study, we showed two constitutive subunits of IL-35 (EBI3 and p35) mRNA and protein were strikingly upregulated in lung tissues from HySu-induced experimental PH mice, and mice serum IL-35 levels were elevated after exposure to HySu. Recent investigations have indicated that IL-35 can be expressed in Tregs, macrophages, and dendritic cells (7,35,36). Concurrent with the results of immunofluorescence staining in the existing research, IL-35 was mainly derived from regulatory T cells, rather than macrophages and dendritic cells, in HySu-induced pulmonary hypertensive mice. In agreement with our observations, Tregs are able to avert the phenotype of PH, suggesting that they may be a key strategy for regulating pulmonary vascular remodeling (21,37). In the complex environment of PH affected lung tissue, the spatial and temporal mediation of different cytokines, chemokines, and growth factors expression may impact Tregs habitation (38), although further studies may be required to prove such potential consequences. Furthermore, by using a pharmacological blockade approach, we explored how IL-35 inhibition or disruption aggravated the development of HySu-induced PH through elevating the RVSP and the thickness of the RV wall, further worsening pulmonary vascular remodeling in mice. These observations suggest that Tregs-derived IL-35 upregulation in lung tissue contributes to pulmonary vascular remodeling associated with PH. It must be noted that using $EBI3^{fl/fl}Foxp3^{cre}$ mice to observe the function of Tregs-derived IL-35 might be beneficial to further validate the observed results in this study. In addition, we revealed that IL-35 neutralization deteriorated the PH in mice by inducing pulmonary arterial EC proliferation. However, PH mice could be attenuated by elevating IL-35 expression, which wielded its function through STAT1 in ECs. These results suggest that the IL-35 signaling pathway specifically affects pulmonary vascular remodeling in PH by modulating conditions for pulmonary EC proliferation.

This study has limitations. Given the lack of tissue and cell samples from PH patients, and with current studies focused only on animal models, it stands to reason that future studies on IL-35 from lung samples in PH patients are required. In summary, we demonstrated that IL-35 can attenuate pulmonary vascular remodeling under PH by reducing pulmonary EC proliferation by enhancing the production of STAT1. Interventions using this immune axis may benefit the management of PH and potentially become a novel therapeutic idea for PH.

Acknowledgments

We thank Dr. Ying Yu (Department of Pharmacology, Key Laboratory of Immune Microenvironment and Disease, School of Basic Medical Sciences, Tianjin Medical University) for generously giving his critical ideas and valuable suggestions. We thank Lin Qiu (Institute for Nutritional Sciences, Shanghai Institutes for Biological Sciences, Chinese Academy of Sciences) for her assistance in flow cytometry.

Funding: This study was supported by a grant to Ankang Lyu from the National Natural Science Foundation of China (NSFC) (81930002, 81770051, and 81570038).

Footnote

Reporting Checklist: The authors have completed the ARRIVE reporting checklist. Available at http://dx.doi.org/10.21037/atm-21-1952

Data Sharing Statement: Available at http://dx.doi.org/10.21037/atm-21-1952

Conflicts of Interest: All authors have completed the ICMJE uniform disclosure form (available at http://dx.doi.org/10.21037/atm-21-1952). The authors have no conflicts of interest to declare.

Ethical Statement: The authors are accountable for all aspects of the work in ensuring that questions related to the accuracy or integrity of any part of the work are appropriately investigated and resolved. All animal experiments were performed under a project license granted by the Animal Ethics Committee of Ruijin Hospital, Shanghai Jiaotong University School of Medicine, China, in compliance with the Animal Ethics Committee of Ruijin Hospital's guidelines for the care and use of animals.

References

1. Coons JC, Pogue K, Kolodziej AR, et al. Pulmonary Arterial Hypertension: a Pharmacotherapeutic Update. Curr Cardiol Rep 2019;21:141.
2. Budhiraja R, Tuder R, Hassoun P. Endothelial dysfunction in pulmonary hypertension. Circulation 2004;109:159-65.
3. Rubin LJ. Pulmonary arterial hypertension. Proc Am Thorac Soc 2006;3:111-5.
4. Lau EMT, Giannoulatou E, Celermajer DS, et al. Epidemiology and treatment of pulmonary arterial hypertension. Nat Rev Cardiol 2017;14:603-14.
5. Wardle AJ, Seager MJ, Wardle R, et al. Guanylate cyclase stimulators for pulmonary hypertension. Cochrane Database Syst Rev 2016;(8):CD011205.
6. Nicolls MR, Voelkel NF. The Roles of Immunity in the Prevention and Evolution of Pulmonary Arterial Hypertension. Am J Respir Crit Care Med 2017;195:1292-9.
7. Collison LW, Workman CJ, Kuo TT, et al. The inhibitory cytokine IL-35 contributes to regulatory T-cell function. Nature 2007;450:566-9.
8. Collison LW, Delgoffe GM, Guy CS, et al. The composition and signaling of the IL-35 receptor are unconventional. Nat Immunol 2012;13:290-9.
9. Vignali DA, Kuchroo VK. IL-12 family cytokines: immunological playmakers. Nat Immunol 2012;13:722-8.
10. Staciwa M, Broncel M. The biological function and significance of IL-35 in the pathogenesis of atherosclerosis. Pol Merkur Lekarski 2018;44:161-4.
11. Mair FM, Wright AF, Duggan N, et al. Sex-dependent influence of endogenous estrogen in pulmonary hypertension. Am J Respir Crit Care Med 2014;190:456-67.
12. Bai P, Lyu L, Yu T, et al. Macrophage-Derived Legumain Promotes Pulmonary Hypertension by Activating the MMP (Matrix Metalloproteinase)-2/TGF (Transforming Growth Factor)-beta1 Signaling. Arterioscler Thromb Vasc Biol 2019:Atvbaha118312254.
13. Lu A, Zuo C, He Y, et al. EP3 receptor deficiency attenuates pulmonary hypertension through suppression of Rho/TGF-beta1 signaling. J Clin Invest 2015;125:1228-42.
14. Jia D, Bai P, Wan N, et al. Niacin Attenuates Pulmonary Hypertension Through H-PGDS in Macrophages. Circ Res 2020;127:1323-36.
15. Calvier L, Boucher P, Herz J, et al. LRP1 Deficiency in Vascular SMC Leads to Pulmonary Arterial Hypertension That Is Reversed by PPAR Activation. Circ Res 2019;124:1778-85.
16. He Y, Zuo C, Jia D, et al. Loss of DP1 Aggravates Vascular Remodeling in Pulmonary Arterial Hypertension via mTORC1 Signaling. Am J Respir Crit Care Med 2020;201:1263-76.
17. Chen G, Zuo S, Tang J, et al. Inhibition of CRTH2-mediated Th2 activation attenuates pulmonary hypertension in mice. J Exp Med 2018;215:2175-95.
18. Yuan K, Shamskhou E, Orcholski M, et al. Loss of Endothelium-Derived Wnt5a Is Associated With Reduced Pericyte Recruitment and Small Vessel Loss in Pulmonary Arterial Hypertension. Circulation 2019;139:1710-24.
19. Ma Z, Yu YR, Badea CT, et al. Vascular Endothelial Growth Factor Receptor 3 Regulates Endothelial Function Through beta-Arrestin 1. Circulation 2019;139:1629-42.
20. Hopper RK, Moonen JR, Diebold I, et al. In Pulmonary Arterial Hypertension, Reduced BMPR2 Promotes Endothelial-to-Mesenchymal Transition via HMGA1 and Its Target Slug. Circulation 2016;133:1783-94.
21. Tamosiuniene R, Tian W, Dhillon G, et al. Regulatory T Cells Limit Vascular Endothelial Injury and Prevent Pulmonary Hypertension. Circ Res 2011;109:867-79.
22. Collison LW, Chaturvedi V, Henderson AL, et al. IL-35-mediated induction of a potent regulatory T cell population. Nat Immunol 2010;11:1093-101.
23. Turnis ME, Sawant DV, Szymczak-Workman AL, et al. Interleukin-35 Limits Anti-Tumor Immunity. Immunity 2016;44:316-29.
24. Evans CE, Cober ND, Dai Z, et al. Endothelial Cells in the Pathogenesis of Pulmonary Arterial Hypertension. Eur Respir J 2021:2003957.
25. Dai Z, Zhu M, Peng Y, et al. Endothelial and Smooth Muscle Cell Interaction via FoxM1 Signaling Mediates Vascular Remodeling and Pulmonary Hypertension. Am J Respir Crit Care Med 2018;198:788-802.
26. Li W, Long L, Yang X, et al. Circulating BMP9 Protects the Pulmonary Endothelium During Inflammation-induced Lung Injury in Mice. Am J Respir Crit Care Med 2021;203:1419-30.

27. Lin J, Kakkar V, Lu X. The role of interleukin 35 in atherosclerosis. Curr Pharm Des 2015;21:5151-9.
28. Jia D, Jiang H, Weng X, et al. Interleukin-35 Promotes Macrophage Survival and Improves Wound Healing After Myocardial Infarction in Mice. Circ Res 2019;124:1323-36.
29. Ciuclan L, Bonneau O, Hussey M, et al. A novel murine model of severe pulmonary arterial hypertension. Am J Respir Crit Care Med 2011;184:1171-82.
30. Abbas A, Gregersen I, Holm S, et al. Interleukin 23 levels are increased in carotid atherosclerosis: possible role for the interleukin 23/interleukin 17 axis. Stroke 2015;46:793-9.
31. Hamaguchi Y, Fujimoto M, Hasegawa M, et al. Bosentan increases serum IL-12 levels in systemic sclerosis patients with pulmonary arterial hypertension. J Dermatol Sci 2009;55:66-7.
32. Qiu HN, Liu B, Liu W, et al. Interleukin-27 enhances TNF-alpha-mediated activation of human coronary artery endothelial cells. Mol Cell Biochem 2016;411:1-10.
33. Huang C, Li Z, Li N, et al. Interleukin 35 Expression Correlates With Microvessel Density in Pancreatic Ductal Adenocarcinoma, Recruits Monocytes, and Promotes Growth and Angiogenesis of Xenograft Tumors in Mice. Gastroenterology 2018;154:675-88.
34. Thenappan T, Ormiston ML, Ryan JJ, et al. Pulmonary arterial hypertension: pathogenesis and clinical management. BMJ 2018;360:j5492.
35. Lee CC, Lin JC, Hwang WL, et al. Macrophage-secreted interleukin-35 regulates cancer cell plasticity to facilitate metastatic colonization. Nat Commun 2018;9:3763.
36. Koda Y, Nakamoto N, Chu P, et al. Plasmacytoid dendritic cells protect against immune-mediated acute liver injury via IL-35. J Clin Invest 2019;129:3201-13.
37. Ulrich S, Nicolls MR, Taraseviciene L, et al. Increased regulatory and decreased CD8+ cytotoxic T cells in the blood of patients with idiopathic pulmonary arterial hypertension. Respiration 2008;75:272-80.
38. Yang B, Wang K, Wan S, et al. TCF1 and LEF1 Control Treg Competitive Survival and Tfr Development to Prevent Autoimmune Diseases. Cell Rep 2019;27:3629-45.e6.

(English Language Editor: B. Draper)

Cite this article as: Wan N, Rong W, Zhu W, Jia D, Bai P, Liu G, Wan Q, Lyu A. Tregs-derived interleukin 35 attenuates endothelial proliferation through STAT1 in pulmonary hypertension. Ann Transl Med 2021;9(11):926. doi: 10.21037/atm-21-1952

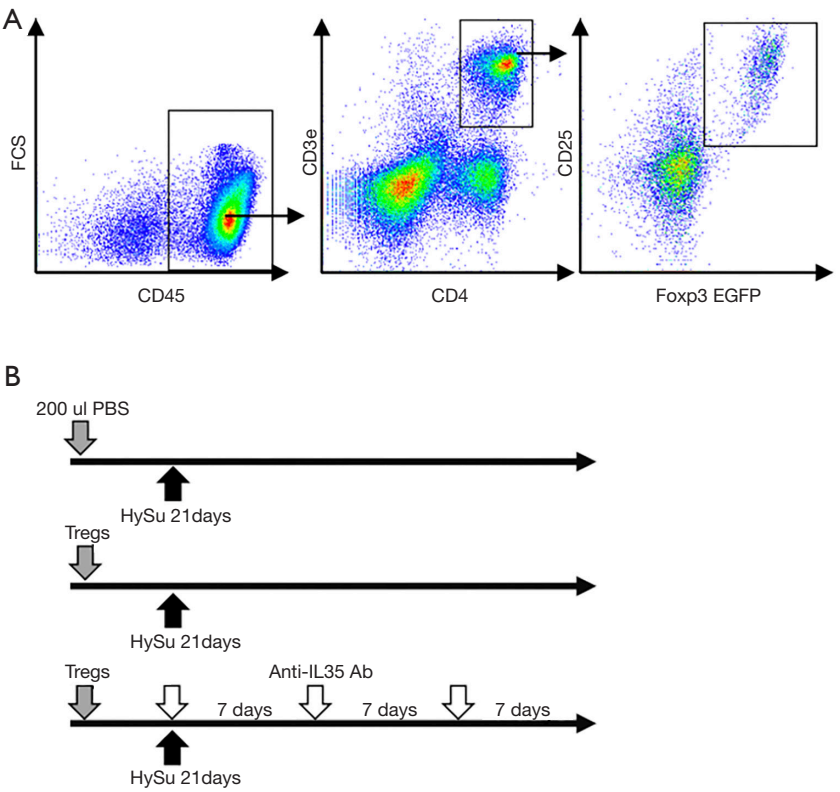

Figure S1 IL-35 mostly derived from Regulatory T cells in PH mice. (A) Gating strategy for Tregs collected from Foxp3^{EGFP} mice spleen were defined as CD45+CD3+CD4+CD25+Foxp3+. (B) Experimental protocol for mice receiving Tregs adoptive transference and weekly administration of IL35 inhibition (100 μg first dose, 50 μg additional doses). PH, pulmonary hypertension.

http://dx.doi.org/10.21037/atm-21-1952

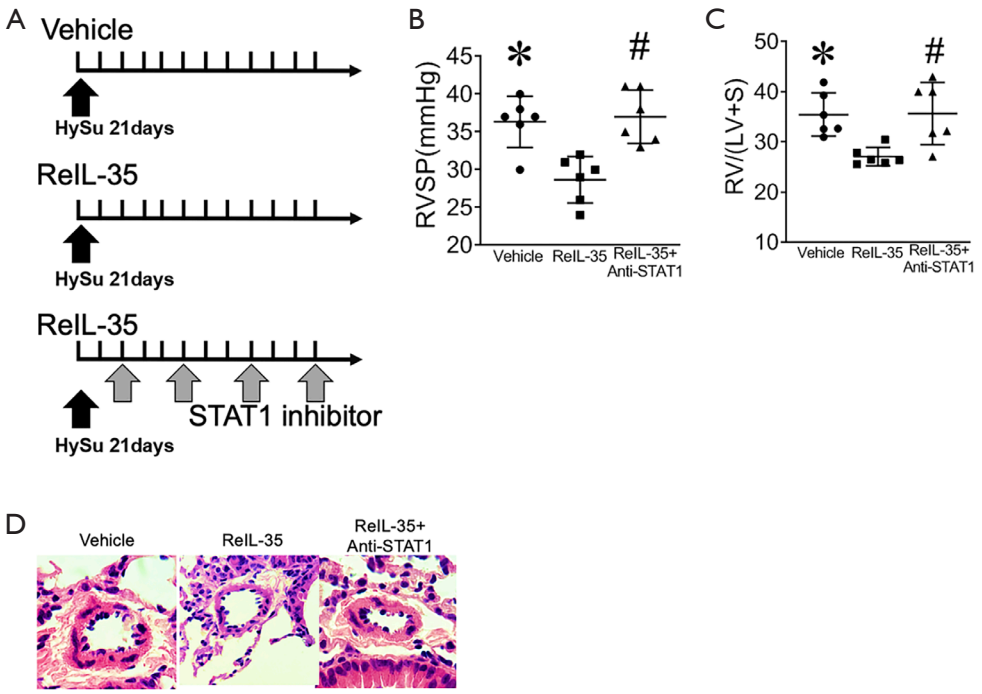

Figure S2 IL-35 abrogates pulmonary EC proliferation through STAT1. (A) Experimental protocol for mice receiving ReIL-35 administration every other day and fludarabine as indicated. (B) Effect of ReIL-35 administration along with both ReIL-35 and fludarabine treatment on right ventricular systolic pressure (RVSP) of HySu-induced mice. *P<0.05 *vs.* vehicle group; #P<0.05 *vs.* vehicle group; n=6 per group. (C) RV/(LV+S) weight ratio in HySu-exposed PH mice with ReIL-35 administration without ReIL-35 administration and with both ReIL-35 and STAT1 inhibition administrated. *P<0.05 *vs.* vehicle group; #P<0.05 *vs.* vehicle group; n=6 per group. (D) Representative images of H&E staining of lung sections from HySu-induced mice with ReIL-35 administration, without ReIL-35 administration, and with both ReIL-35 and STAT1 inhibition administrated. Scale bar: 20 μm. EC, endothelial cell. HySu, hypoxia plus SU5416. ReIL-35, recombinant IL-35.

http://dx.doi.org/10.21037/atm-21-1952